Computers & Fluids 111 (2015) 69–75

Contents lists available at ScienceDirect

Computers & Fluids

journal homepage: www.elsevier.com/locate/compfluid

Application of the HAM-based Mathematica package BVPh 2.0 on MHD Falkner–Skan flow of nano-fluid

U. Farooq [a,d], Y.L. Zhao [a], T. Hayat [b,c], A. Alsaedi [b], S.J. Liao [a,b,*]

[a] State Key Laboratory of Ocean Engineering, School of Naval Architecture, Ocean and Civil Engineering, Shanghai Jiao Tong University, Shanghai 200240, China
[b] Nonlinear Analysis and Applied Mathematics (NAAM) Research Group, Faculty of Science, King Abdulaziz University, Jeddah 21589, Saudi Arabia
[c] Department of Mathematics, Quaid.i.Azam University, Islamabad 44000, Pakistan
[d] Comsats Institute of Information Technology (CIIT), Park Road Chak Shahzad, Islamabad, Pakistan

ARTICLE INFO

Article history:
Received 17 March 2014
Received in revised form 6 January 2015
Accepted 9 January 2015
Available online 29 January 2015

Keywords:
Falkner–Skan flow
MHD
Nanofluid
Homotopy analysis method
BVPh 2.0

ABSTRACT

Many boundary-layer flows are governed by one or coupled nonlinear ordinary differential equations (ODEs). Currently, a Mathematica package BVPh 2.0 is issued for nonlinear boundary-value/eigenvalue problems with boundary conditions at multiple points. The BVPh 2.0 is based on an analytic approximation method for highly nonlinear problems, namely the homotopy analysis method (HAM), and is free available online. In this paper, the BVPh 2.0 is successfully applied to solve magnetohydrodynamic (MHD) Falkner–Skan flow of nano-fluid past a fixed wedge in a semi-infinite domain, and the influence of physical parameters on the considered flows is investigated in details. Physically, this work deepens and enriches our understandings about the magnetohydrodynamic Falkner–Skan flows of nano-fluid past a wedge. Mathematically, it illustrates the potential and validity of the BVPh 2.0 for complicated boundary-layer flows.

1. Introduction

In fluid mechanics, the Falkner–Skan flow is significant and fundamental in both theory and practice. In particular, such kind of flows occur frequently in enhanced oil recovery, packed bed reactor geothermal industries, etc. Moreover, there is growing interest of the researchers in the magnetohydrodynamics (MHD) flows, mainly due to their vast applications in power generators, design of heat exchangers, electrostatic filters, the cooling of reactor, MHD accelerators and so on. The magnetic field has also stabilizing effects in this kind of boundary layer flows. Hence, many researchers have been doing their contributions to the Falkner–Skan flows with or without a magnetic field. For example, Abbasbandy and Hayat [1,2] analyzed the MHD Falkner–Skan flow of viscous fluid using the homotopy analysis and Hankel–Pade methods. Parand et al. [3] developed approximate solution of MHD Falkner–Skan flow by the Hermite functions pseudo-spectral method. The solutions of reversed flow of the Falkner–Skan equations were obtained by Yang and Lan [4]. Yao [5,6] examined the uniform suction and heat transfer influences in the Falkner–Skan wedge flow. The generalized Falkner–Skan equations in the FENE fluid was investigated by Anabtawi and Khuri [7]. The numerical solutions of the Falkner–Skan equations in viscous fluid were gained by Zhu et al. [8]. The Falkner–Skan flow due to stretching surface was addressed by Yao and Chen [9]. Alizadeh et al. [10] obtained the solutions of Falkner–Skan equation with wedge using the Adomian decomposition method.

Nano-particles are objects with at least one dimension smaller than 100 nm (preferably <10 nm), where a nanometer (nm) is one-billionth of a meter. Although nano-particles are so small, they often possess far more remarkable characteristics than the same material and bulk without them. Fluids such as oil, water and ethylene glycol mixtures are naturally poor in heat transfer. In the past decades, lots of researches were done to develop fluids with ultrahigh-performance such as the enhanced electrical conductivity, intensified heat transfer, improved oils, coolants and industrial equipments. When a very small amount of nano-particles are dispersed uniformly and suspended stably in clear fluids, the thermal properties of the fluid changes significantly. Choi [11] called these fluids as nano-fluids, and proposed that nanometer-sized metallic particles can be suspended in industrial heat transfer fluids. Therefore, a nano-fluid is a suspension of nano-particles in a traditional base fluid, which enhances the heat transfer characteristics of the

* Corresponding author at: State Key Laboratory of Ocean Engineering, School of Naval Architecture, Ocean and Civil Engineering, Shanghai Jiao Tong University, Shanghai 200240, China.

E-mail address: sjliao@sjtu.edu.cn (S.J. Liao).

http://dx.doi.org/10.1016/j.compfluid.2015.01.005
0045-7930/

clear fluid. Nano-technology has applications in automatize industry, electronic devices, such as supercomputers, cooling systems, power plants, and artificial organs. Choi et al. [12] observed that the thermal conductivity of fluid can be increased up to approximately two times by means of adding a small amount (less then 1%) of nano-particles to clear liquids. For reviews on nano-fluids, please refer to Das et al. [13] and Wang and Mujundar [14]. Recently, the Falkner–Skan problem for a static or moving wedge in hydrodynamic viscous nano-fluids has been numerically investigated by Yacob et al. [15] and Fallah et al. [16]. They gained the Pareto optimal solutions by means of multi-objective genetics algorithms. Khan et al. [17] numerically examined the Falkner–Skan boundary layer flow of nano-fluid over wedge with convective boundary condition. Khan and Pop [18] considered steady boundary-layer flows past a stretching wedge in a viscous nano-fluid with a parallel free stream velocity $u_e(x)$.

In this paper, a steady-state laminar two dimensional MHD boundary layer flow of viscous nano-fluid past a fixed wedge is considered. The magneto nano-fluids are important in applications related to modulators, optical switches, optical gratings, tunable optical fiber filters and so on. The magnetic nano-particles are important in medicine, sink float separation, cancer therapy, magnetic cell separation, construction of loud speakers, magnetic resonance imaging and so on. In the form of the boundary-layer theory, the considered problem is governed by three coupled nonlinear ordinary differential equations (ODEs) in a semi-infinite domain with boundary conditions at infinity. Traditionally, such kind of coupled nonlinear ODEs can be solved by means of numerical methods such as the finite difference method (FDM) by means of moving the boundary condition at infinity to a finite but far enough position which causes some uncertainty and inaccuracy to its numerical solutions. Unlike the traditional approaches, we use here a Mathematica package BVPh 2.0 [19] for nonlinear boundary-value/eigenvalue problems governed by coupled nonlinear ODEs with multiple boundary conditions, which can exactly satisfy the boundary condition at infinity, since the BVPh 2.0 is based on the computer algebra system Mathematica and makes computations with functions instead of numbers. Mathematically, the BVPh 2.0 is based on the homotopy analysis method (HAM) [20–23], an analytic approximation technique for highly nonlinear problems and has many advantages compared to the traditional ones. First, based on the homotopy in topology, the HAM can always transfer a nonlinear problem into an infinite number of linear sub-problems without any small/large physical parameters, and besides provides us great freedom to choose the equation-type and base function of solution of these linear sub-problems for high-order approximations. Especially, unlike all other analytic approximation methods, the HAM provides us a simple way to guarantee the convergence of solution series, so that it is valid for problems with high nonlinearity. The general validity and power of the HAM have been illustrated by hundreds of successful applications of the HAM in various fields of science, finance and engineering. To simplify the applications of the HAM, some HAM-based packages in Mathematica or Maple have been developed. The BVPh 2.0 is one of them, which is an easy-to-use tool for boundary-layer flows, and is free available online (http://numericaltank.sjtu.edu.cn/BVPh.htm).

In this paper, the BVPh 2.0 is used to solve the considered magnetohydrodynamics (MHD) Falkner–Skan flow of nano-fluid. The influence of physical parameters on the profiles of velocity, temperature and concentration, the local skin friction coefficient, the local Nusselt number and the local Sherwood number is investigated in details. Physically, this work deepens and enriches our understandings about the magnetohydrodynamics (MHD) Falkner–Skan flow of nano-fluid. Mathematically, it illustrates that the HAM-based Mathematica package is indeed an easy-to-use tool for complicated boundary-layer flows.

2. Mathematical formulas

We consider here a steady-state laminar incompressible two dimensional boundary-layer flow of nano-fluid past a fixed wedge. A constant magnetic field of strength B acts in a transverse direction to flow. The fluid is electrically conducting in the presence of applied magnetic field B. The induced magnetic field effect is not taken into account. Such consideration holds when magnetic Reynolds number is chosen small. In addition the influence of electric field is negligible. In this situation the current density becomes $\bar{J} = \sigma(\overline{V} \times \overline{B})$ and lorentz force $\bar{J} \times \overline{B} = -\sigma B^2 V$. In-fact zero electric field corresponds to the case when polarization effects are not considered. The Hall effect is also not taken into account. Let T_w, C_w and T_∞, C_∞ denote the temperature and concentration at the surface and at infinity, respectively. Effects of Brownian motion and thermophoresis are considered. Under these assumptions, the governing equations of continuity, momentum, energy and nanoparticle volume fraction are as follows (see Fig. 1):

(i) Continuity equation

$$\frac{\partial u}{\partial x} + \frac{\partial v}{\partial y} = 0. \tag{1}$$

(ii) Equation of motion

$$u\frac{\partial u}{\partial x} + v\frac{\partial u}{\partial y} = U\frac{dU}{dx} + \nu\frac{\partial^2 u}{\partial y^2} - \frac{\sigma B^2}{\rho_f}(u - U). \tag{2}$$

(iii) Energy equation

$$u\frac{\partial T}{\partial x} + v\frac{\partial T}{\partial y} = \alpha\frac{\partial^2 T}{\partial y^2} + \tau\left\{D_B\left(\frac{\partial C}{\partial y}\frac{\partial T}{\partial y}\right) + \frac{D_T}{T_\infty}\left(\frac{\partial T}{\partial y}\right)^2\right\}. \tag{3}$$

(iv) Nanoparticle volume fraction equation

$$u\frac{\partial C}{\partial x} + v\frac{\partial C}{\partial y} = D_B\left(\frac{\partial^2 C}{\partial y^2}\right) + \frac{D_T}{T_\infty}\left(\frac{\partial^2 T}{\partial y^2}\right), \tag{4}$$

where u, v are the x- and y-components of the fluid velocity, U denotes the inherent characteristic velocity, T the temperature, α the thermal diffusivity, τ the ratio of heat capacity of nano-particle to that of the base fluid, ν the kinematic viscosity, σ the electrical conductivity, K the thermal conductivity, T_∞ and C_∞ the free stream temperature and concentration, C the nano-particle volume fraction, D_B the Brownian diffusion coefficient, D_T the thermophoretic diffusion coefficient and ρ_f the fluid density, respectively. The corresponding initial and boundary conditions are

$$u = 0, \quad v = 0, \quad T = T_w, \quad C = C_w(x) \quad \text{at} \quad y = 0, \tag{5}$$

$$u = U(x) = ax^n, \quad T \to T_\infty, \quad C \to C_\infty \quad \text{as} \quad y \to \infty. \tag{6}$$

with

$$B = B_0 x^{(n-1)/2}, \tag{7}$$

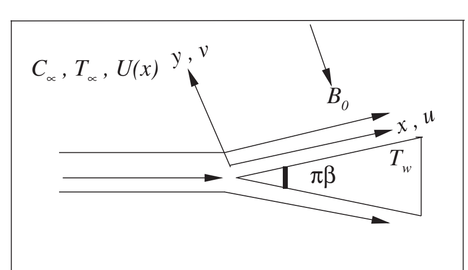

Fig. 1. Physical configuration.

where x is the distance from the leading edge, n the Falkner–Skan power-law parameter, T_w the surface temperature distribution, T_∞ the ambient fluid temperature distribution, and C_∞ the ambient fluid nano-particle volume fraction, respectively. Using the similarity transformations [1]

$$u = U(x)f', \quad \eta = \sqrt{\frac{n+1}{2}}\sqrt{\frac{U}{\nu x}}y, \quad \psi = \sqrt{\frac{2}{n+1}}\sqrt{\nu x U}f(\eta),$$
$$v = -\sqrt{\frac{n+1}{2}}\sqrt{\frac{\nu U}{x}}\left[f(\eta) + \frac{n-1}{n+1}\eta f'(\eta)\right], \quad \theta(\eta) = \frac{T - T_\infty}{T_w - T_\infty}, \tag{8}$$
$$\phi(\eta) = \frac{C - C_\infty}{C_w - C_\infty},$$

where $\nu\left(=\frac{\mu}{\rho_f}\right)$ is the kinematic viscosity and μ is the dynamic viscosity, we have the non-dimensional governing equations (after dropping asterisks):

$$\mathcal{N}_f(f) = f''' + ff'' + \beta(1 - f'^2) - M^2(f' - 1) = 0, \tag{9}$$
$$\mathcal{N}_\theta(f, \theta, \phi) = \theta'' + Pr(f\theta' + N_t\theta'^2 + N_b\theta'\phi') = 0, \tag{10}$$
$$\mathcal{N}_\phi(f, \theta, \phi) = \phi'' + PrLef\phi' + \frac{N_t}{N_b}\theta'' = 0, \tag{11}$$

where $\mathcal{N}_f(f), \mathcal{N}_\theta(f,\theta,\phi), \mathcal{N}_\phi(f,\theta,\phi)$ are nonlinear differential operators defined above. Here, M, Pr, N_b, N_t and Le are the so-called magnetic field parameter, the Prandtl number, the Brownian motion parameter, the thermophoresis parameter, and the Lewis number, respectively, defined by

$$M^2 = \frac{2\sigma B_0^2}{\rho_f a(1+n)}, \quad N_b = \frac{\tau(C_w - C_\infty)D_B}{\nu}, \tag{12}$$
$$N_t = \frac{\tau D_T(T_w - T_\infty)}{\nu T_\infty}, \quad Le = \frac{\alpha}{D_B}, \quad Pr = \frac{\nu}{\alpha}, \quad \beta = \frac{2n}{n+1}. \tag{13}$$

The corresponding non-dimensional boundary conditions are given by

$$\left.\begin{array}{l} f(0) = 0, \quad f'(0) = 0, \quad f'(+\infty) = 1, \\ \theta(0) = 1, \quad \theta(+\infty) = 0, \quad \phi(0) = 1, \quad \phi(\infty) = 0. \end{array}\right\} \tag{14}$$

It should be pointed out that the case of $n > 0$ and $\beta > 0$ corresponds to a wedge in an accelerated flow, whereas decelerated flow with separation occurs in the case of $n < 0$ and $\beta < 0$.

The parameters with physical interests, such as the skin friction coefficient C_{fx}, the local Nusselt number Nu_x and the local Sherwood number Sh_x, are defined as follows:

$$C_{fx} = \frac{\tau_{wx}}{\rho U_w^2}, \quad Nu_x = \frac{xq_w}{K(T_w - T_\infty)} \quad Sh_x = \frac{xj_w}{D_B(C_w - C_\infty)}, \tag{15}$$

where τ_w, q_w and j_w are the wall skin friction, the heat flux and the mass flux from the surface, respectively, defined by

$$\tau_{wx} = \mu\left(\frac{\partial u}{\partial y}\right)_{y=0}, \quad q_w = -K\left(\frac{\partial T}{\partial y}\right)_{y=0} \quad j_w = -D_B\left(\frac{\partial C}{\partial y}\right)_{y=0}. \tag{16}$$

According to (8), we have the non-dimensional local skin friction coefficient, the local Nusselt number and the local Sherwood number

$$(Re)^{\frac{1}{2}}C_{fx}\sqrt{\frac{2}{n+1}} = f''(0), \quad (Re)^{-\frac{1}{2}}Nu_x\sqrt{\frac{2}{n+1}} = -\theta'(0),$$
$$(Re)^{-\frac{1}{2}}Sh_x\sqrt{\frac{2}{n+1}} = -\phi'(0), \tag{17}$$

where $Re = (Ux)/\nu$ is the local Reynolds number.

3. Analytic approximations given by the BVPh 2.0

The system of the coupled nonlinear ODEs (9)–(11) with the boundary conditions (14) can be solved by means of the BVPh 2.0, a HAM-based Mathematica package [19] for coupled nonlinear ODEs with multiple boundary conditions in finite or infinite domains. The BVPh 2.0 is free available online (http://numerical-tank.sjtu.edu.cn/BVPh.htm) with a simple user's guide.

The BVPh 2.0 is easy-to-use: one only need define the governing equations and boundary conditions under consideration, then choose an auxiliary linear operator for each governing equation, which defines the equation-type of the corresponding high-order equations, and a proper initial guess for each unknown function. With these inputs, the BVPh 2.0 automatically gives you the analytic approximations at whatever order you would like. Note that there exist a convergence-control parameter for each governing equation, which is used to guarantee the convergence of series solution. The optimal values of the convergence-control parameters are determined by the minimum of residual squares of governing equations (and also boundary conditions in some cases).

Thus HAM which is based on the homotopy in topology, transfers a nonlinear problem into an infinite number of linear sub-problems, but without any small/large physical parameters. For the considered problem, we have

$$f(\eta) = \sum_{k=0}^{+\infty} f_k(\eta), \quad \theta(\eta) = \sum_{k=0}^{+\infty} \theta_k(\eta), \quad \phi(\eta) = \sum_{k=0}^{+\infty} \phi_k(\eta), \tag{18}$$

where $f_k(\eta), \theta_k(\eta), \phi_k(\eta)$ are determined by the so-called high-order deformation equations governed by the chosen auxiliary linear operators. According to Eqs. (9)–(11) and the boundary conditions (14) at infinity, it is obvious that $f(\eta), \theta(\eta), \phi(\eta)$ should be in the forms:

$$f(\eta) = A_{0,0}^k + \sum_{k=0}^{+\infty}\sum_{j=1}^{+\infty}\sum_{i=0}^{+\infty} A_{i,j}^k \eta^i \exp(-j\eta),$$
$$\theta(\eta) = \sum_{k=0}^{+\infty}\sum_{j=1}^{+\infty}\sum_{i=0}^{+\infty} B_{i,j}^k \eta^i \exp(-j\eta), \tag{19}$$
$$\phi(\eta) = \sum_{k=0}^{+\infty}\sum_{j=1}^{+\infty}\sum_{i=0}^{+\infty} C_{i,j}^k \eta^i \exp(-j\eta),$$

where $A_{i,j}^k, B_{i,j}^k$ and $C_{i,j}^k$ are constant coefficients to be determined by the BVPh 2.0. Eq. (19) represents the so called "solution expressions", which provide us a guide to choose the auxiliary linear operator and initial guess, and thus play an important role in the HAM.

In the frame of HAM, one has great freedom to choose the auxiliary linear operators. According to the above-mentioned solution expression, we could choose the following auxiliary linear operators:

$$\mathcal{L}_1[f(\eta:q)] = \frac{d^3 f}{d\eta^3} + \gamma\frac{d^2 f}{d\eta}, \tag{20}$$
$$\mathcal{L}_2[\theta(\eta:q)] = \frac{d^2\theta}{d\eta^2} + \frac{d\theta}{d\eta}, \tag{21}$$
$$\mathcal{L}_3[\phi(\eta:q)] = \frac{d^2\phi}{d\eta^2} + \frac{d\phi}{d\eta}, \tag{22}$$

which have the following properties

$$\mathcal{L}_1[C_1\exp(-\eta) + C_2\exp(\eta) + C_3] = 0, \tag{23}$$
$$\mathcal{L}_2[C_4\exp(-\eta) + C_5\exp(\eta)] = 0, \tag{24}$$
$$\mathcal{L}_3[C_6\exp(-\eta) + C_7\exp(\eta)] = 0, \tag{25}$$

where $C_1, C_2, \ldots, C_7$ are constants to be determined by the boundary conditions.

In the frame of the HAM, we also have great freedom to choose the initial approximations. According to the above-mentioned solution expression and the boundary conditions (14), we choose the following initial approximations:

$$f_0(y) = \eta - \frac{1 - \exp(-\gamma\eta)}{\gamma}, \tag{26}$$

$$\theta_0(y) = \exp(-\eta), \tag{27}$$

$$\phi_0(y) = \exp(-\eta), \tag{28}$$

where $\gamma = 2$. It should be noticed that initial approximations must satisfy the boundary conditions (14). These are enough for the BVPh 2.0: using the auxiliary linear operator (20)–(22) and the initial approximations (26)–(28), analytic approximations of the coupled nonlinear ODEs (9)–(11) with the boundary conditions (14) can be gained automatically by the BVPh 2.0.

It should be emphasized that $f(\eta), \theta(\eta)$ and $\phi(\eta)$ given by the BVPh 2.0 contain three unknown convergence-control parameters c_0^f, c_0^θ and c_0^ϕ, which are used to guarantee the convergence of the series solutions. It should be noticed that the convergence-control parameters play very important role in the frame of the HAM: it is the so-called convergence-control parameter that differs the HAM from all other analytic approximation methods.

To greatly decrease the CPU time, we use here the so-called average residual error at the kth-order of approximation, defined by

$$\mathcal{E}_k^f(c_0^f, c_0^\theta, c_0^\phi) = \frac{1}{N+1}\sum_{j=0}^{N}\left[\mathcal{N}_f\left(\sum_{i=0}^{k} f_i\right)\Bigg|_{\eta=j\delta\eta}\right]^2, \tag{29}$$

$$\mathcal{E}_k^\theta(c_0^f, c_0^\theta, c_0^\phi) = \frac{1}{N+1}\sum_{j=0}^{N}\left[\mathcal{N}_\theta\left(\sum_{i=0}^{k} f_i, \sum_{i=0}^{k}\theta_i, \sum_{i=0}^{k}\phi_i\right)\Bigg|_{\eta=j\delta\eta}\right]^2, \tag{30}$$

$$\mathcal{E}_k^\phi(c_0^f, c_0^\theta, c_0^\phi) = \frac{1}{N+1}\sum_{j=0}^{N}\left[\mathcal{N}_\phi\left(\sum_{i=0}^{k} f_i, \sum_{i=0}^{k}\theta_i, \sum_{i=0}^{k}\phi_i\right)\Bigg|_{\eta=j\delta\eta}\right]^2, \tag{31}$$

for the original governing equations, respectively. Where N is an integer. The total error at the kth-order of approximation is defined by

$$\mathcal{E}_k^t(c_0^f, c_0^\theta, c_0^\phi) = \mathcal{E}_k^f(c_0^f, c_0^\theta, c_0^\phi) + \mathcal{E}_k^\theta(c_0^f, c_0^\theta, c_0^\phi) + \mathcal{E}_k^\phi(c_0^f, c_0^\theta, c_0^\phi). \tag{32}$$

Note that all boundary conditions are linear and are exactly satisfied. At the kth-order of approximation, the optimal values of $c_0^f, c_0^\theta, c_0^\phi$ are determined by the minimum of the total error $\mathcal{E}_k^t$, which can be done simply using "**GetOptiVar**", a command of the BVPh 2.0. For details, please refer to the user's guide of the BVPh 2.0 online (http://numericaltank.sjtu.edu.cn/BVPh.htm).

4. Results and discussion

Without loss of generality, let us consider the case $\beta = M = N_b = N_t = 0.1, Le = 1.0$ and $Pr = 7.0$. The corresponding optimal convergence-control parameters are gained by directly employing the command "**GetOptiVar**" of the BVPh 2.0, which are listed in Table 1 for up to the 6th-order of approximations. Note that the total error $\mathcal{E}_k^t$ decreases to 9.6×10^{-3} by means of the corresponding optimal convergence-control parameters $c_0^f = -1.37$, $c_0^\theta = -1.03, c_0^\phi = -0.99$. It is found that, using these optimal convergence-control parameters gained at the 6th-order of approximation, the residual error of each governing equation indeed decreases, as shown in Table 2. In this way, we gain the convergent analytic solution for the considered problem in the case mentioned above.

Similarly, one can gain the convergent analytic approximations for different physical parameters by means of the BVPh 2.0. For example, the local skin friction coefficients $f''(0)$ for different wedge angle β in the case of $M = 0$ agree well with those reported by Yacob et al. [15], Khan and Pop [18], Yih [24] and White [25], as shown in Table 3. This illustrates the validity of the BVPh 2.0 for the considered boundary-layer flows of nano-fluid.

Figs. 2–11 depict the features of velocity, temperature and concentration profiles as a function of η for various wedge angles (β), magnetic fields (M), Brownian motion parameters (N_b), thermophoresis parameters (N_t), Lewis numbers (Le) and the Prandtl numbers (Pr), respectively. The quantities describing the momentum, heat and mass transfer i.e. the local skin friction coefficient, the local Nusselt number and the local Sherwood number at the leading edge have been plotted for various values of the physical parameters.

Figs. 2 and 3 depicts the influence of β and M on the velocity, temperature and concentration profiles. It is found that the increase in β and M results in an increase in the velocity profile, whereas the rate of convergence to the mainstream flow decreases. Besides, the increase in either β and M decreases the velocity boundary layer thickness. The increase of β leads to the decrease of the thermal and concentration profiles in the boundary layer regions.

The continuous collision between the nano-particles and the base fluid molecules generates a random motion of nano-particles within base fluid, called the Brownian motion. The influence of the Brownian motion parameter N_b on the temperature and concentration profiles for a fixed wedge is shown in Figs. 4 and 5. As shown in Fig. 4, the increase in N_b with $\beta = 0.1$ or $\beta = 1.0$ (keeping all other parameters fixed) leads to the increase of the temperature profiles in the boundary layer region. However, the increase in β decreases the temperature in the thermal boundary layer region. As shown in Fig. 5, the concentration profile decreases in the boundary layer with an increase in the Brownian motion parameter. Besides, the concentration profile decays more quickly for larger values of N_b. The increase in β results in the decrease of the concentration profile.

Figs. 6 and 7 show the variations of the temperature and nano-particle volume fraction with N_t for various values of β. It is found that the temperature profiles increase by increasing the thermophoretic parameter. A significant change is noticed in the nano-particle volume fraction for various values of N_t. For $N_t = 0.1$, the concentration profile is a decreasing function of η. However, increasing N_t, the concentration profile first increases and attains the maximum value in the ambient fluid near the surface and then asymptotically approaches to zero.

Table 1
Optimal convergence-control parameters at different orders of approximation in the case of $\beta = M = N_b = N_t = 0.1, Le = 1$ and $Pr = 7.0$.

k (order of approximation)	c_0^f	c_0^θ	c_0^ϕ	$\mathcal{E}_k^t$
1	−0.75	−0.64	−0.59	2.4×10^{-1}
3	−1.18	−0.77	−0.83	6.7×10^{-2}
6	−1.37	−1.03	−0.99	9.6×10^{-3}

Table 2
Average squared residual errors at different orders of approximation in the case of $\beta = M = N_b = N_t = 0.1, Le = 1$ and $Pr = 7.0$ by means of the optimal convergence-control parameters $c_0^f = -1.37, c_0^\theta = -1.03, c_0^\phi = -0.99$.

k (order of approximation)	10	20	30
$\mathcal{E}_k^f$	3.7×10^{-4}	3.1×10^{-5}	4.5×10^{-6}
$\mathcal{E}_k^\theta$	4.0×10^{-4}	1.5×10^{-5}	1.1×10^{-6}
$\mathcal{E}_k^\phi$	1.0×10^{-3}	4.6×10^{-5}	4.0×10^{-6}
$\mathcal{E}_k^t$	1.8×10^{-3}	9.3×10^{-5}	9.7×10^{-6}

Table 3
Comparison of $f''(0)$ given by the BVPh 2.0 with the previous publications when $M = 0$.

β	Yih [24]	Yacob et al. [15]	White [25]	Khan and Pop [18]	HAM
0	0.4696	0.4696	0.4696	0.4696	0.4696
1/6	0.6550	0.6550	0.6550	0.6550	0.6550
1/3	0.8021	0.8021	0.8021	0.8021	0.8021
1/2	0.9276	0.9276	0.9277	0.9277	0.9276
2/3	–	–	1.0389	1.0389	1.0389
1	–	1.2326	1.2326	1.2326	1.2326

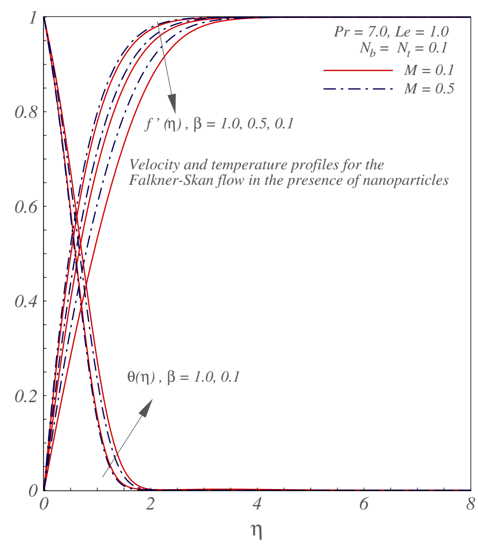

Fig. 2. Velocity and temperature profile for different values of β and M.

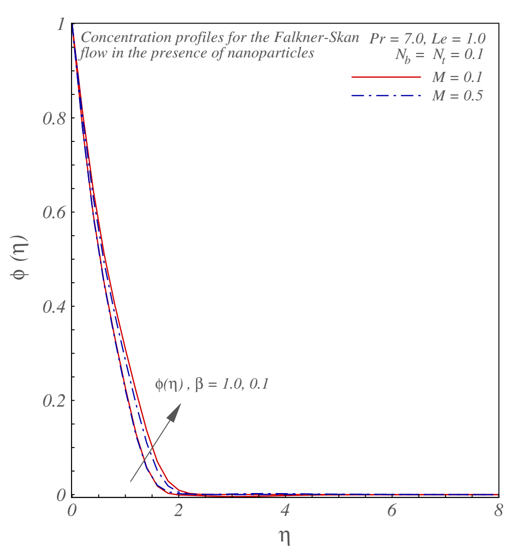

Fig. 3. Concentration profile for different values of β and M.

Figs. 8 and 9 show the variations of temperature and concentration profiles with Prandtl number for various values of β. It is found that temperature and concentration profile is a decreasing function of Prandtl number. Physically, the increase of Prandtl number leads to the decrease of the thermal diffusivity which results in low thermal conduction and hence the decrease of the temperature.

Fig. 10 presents the influence of the Lewis number for various of β on the concentration profile. The concentration profile is a

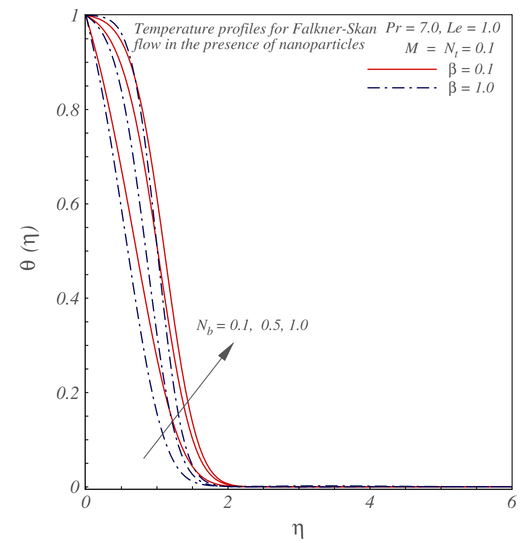

Fig. 4. Graphs of $\theta(\eta)$ for different N_b with various β.

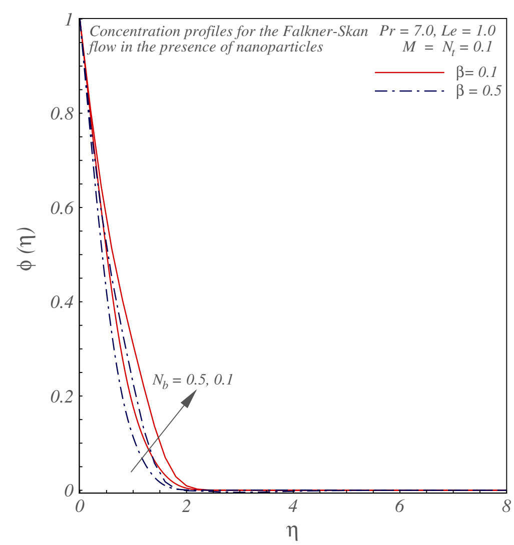

Fig. 5. Graphs of $\phi(\eta)$ for different N_b with various β.

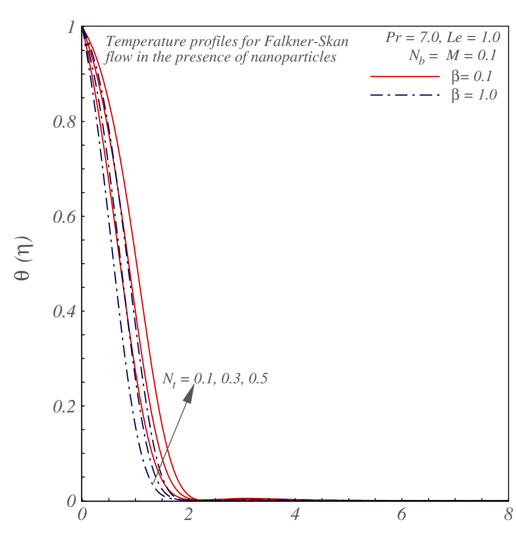

Fig. 6. Graphs of $\theta(\eta)$ for different N_t with various β.

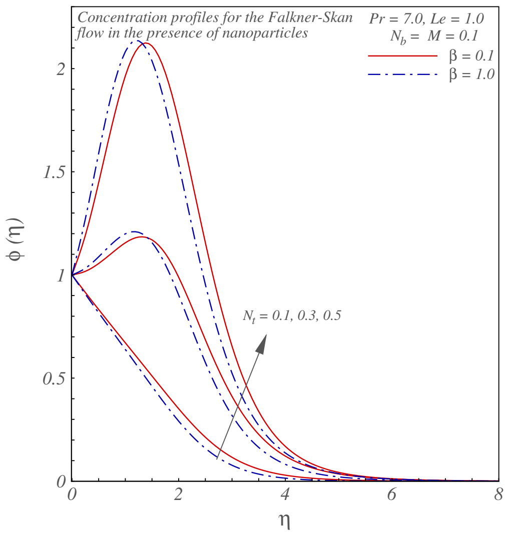

Fig. 7. Graphs of $\phi(\eta)$ for different N_t with various β.

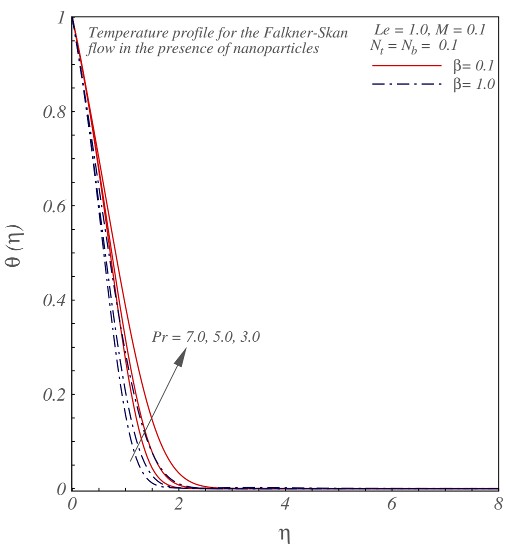

Fig. 8. Graphs of $\theta(\eta)$ for different Pr with various β.

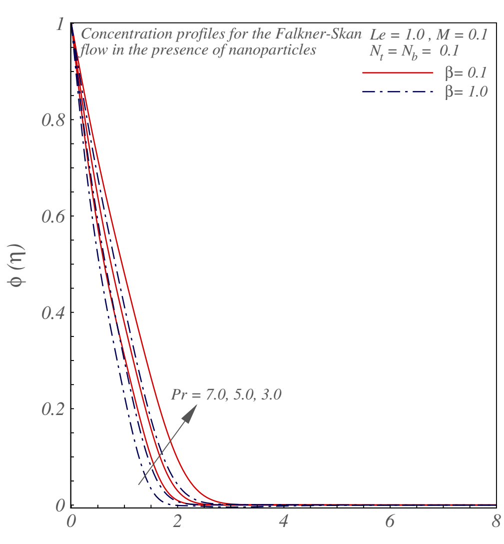

Fig. 9. Graphs of $\phi(\eta)$ for different Pr with various β.

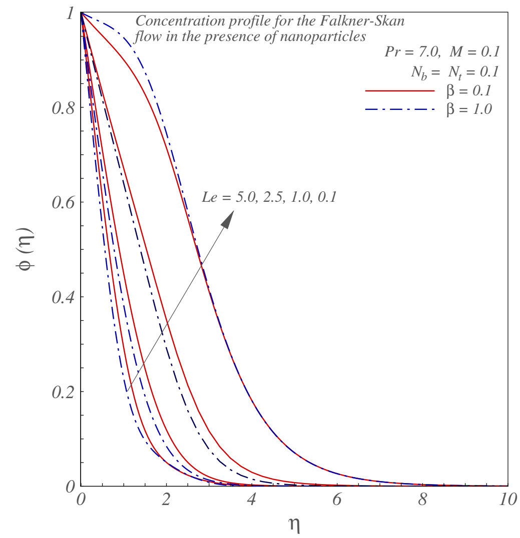

Fig. 10. Graphs of $\phi(\eta)$ for different Le with various β.

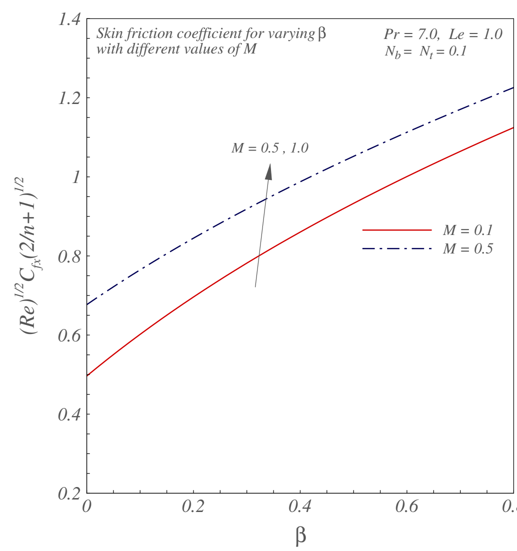

Fig. 11. Skin friction coefficient versus β.

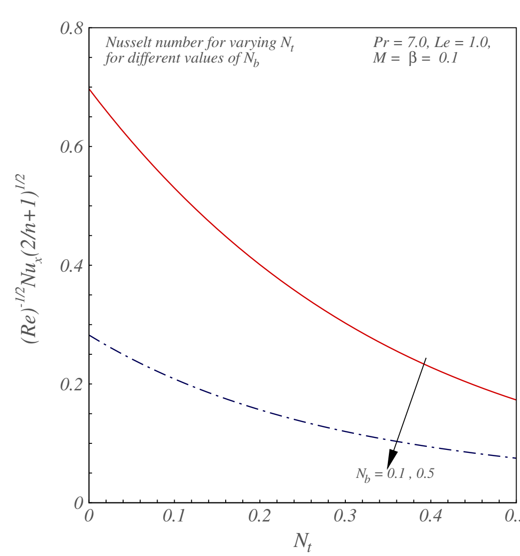

Fig. 12. Nusselt number versus N_t.

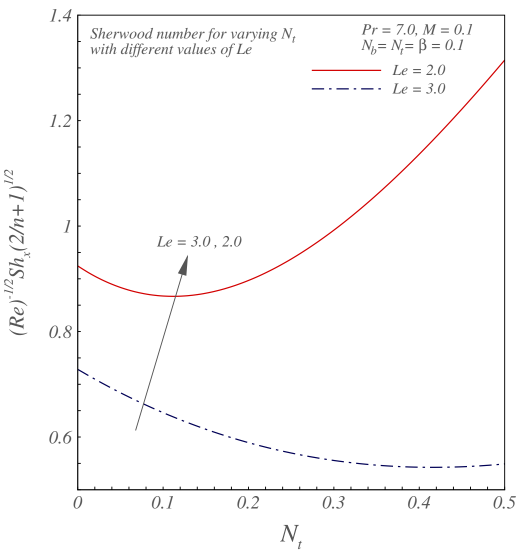

Fig. 13. Sherwood number versus N_t.

decreasing function of the Lewis number. It is due to the fact that the increase in Lewis number leads to the decrease of the molecular diffusivity.

The local skin friction coefficient at the leading edge against β is shown in Fig. 11 for various values of M. It is found the local skin friction increases with the increase in β and M.

Fig. 12 examines the local Nusselt number at the leading edge. The Nusselt number is plotted as function of N_t. It is found that the Nusselt number is a decreasing function of N_t also the increase in N_b leads to the decrease of the Nusselt number.

According to Fig. 13, the local Sherwood number decreases with the increase in Le. We already noticed in Fig. 10 that the concentration boundary layer thickness decreases with the increase in N_b and Le, such decrease in fact is responsible for the decrease in the mass transfer.

5. Conclusions

In this paper, a steady-state laminar two dimensional MHD boundary layer flow of nano-fluid past a fixed wedge is investigated in details. Mathematically, the HAM-based Mathematica package BVPh 2.0 is used to solve the corresponding system of three coupled nonlinear ODEs defined in a semi-infinite domain. Unlike numerical approaches, the BVPh 2.0 exactly satisfies the boundary conditions at infinity. Besides, based on the HAM, the BVPh 2.0 provides us a simple way to guarantee the convergence of solution series by means of the so-called optimal convergence-control parameters. Thus, the HAM-based Mathematica package BVPh 2.0, which is free available online (http://numericaltank.sjtu.edu.cn/BVPh.htm) with a user's guide, is indeed an easy-to-use tool for some complicated boundary-layer flows.

Physically, the influence of physical parameters on the MHD Falkner–Skan boundary-layer flows of nano-fluid is studied in details. It is found that:

(1) Fluid flow enhances with the increase of β and M.
(2) Temperature increases with the increase of N_b, N_t but decreases for Pr.
(3) Concentration profile decreases with the increase of N_b, Le but increases with the increase of N_t.
(4) The local skin friction coefficient increases with the increase of β but decreases with the increase in M.
(5) The increase in N_b decreases the heat transfer.
(6) The mass transfer decreases with the increase of Le.

These results deepen and enrich our understandings about the MHD boundary layer flows of nano-fluid past a fixed wedge.

Acknowledgements

This work is supported in part by State Key Laboratory of Ocean Engineering (Approval No. GKZD010063) and National Natural Science Foundation of China (Approval Nos. 11272209 and 51209136). The research of Dr. Alsaedi is partially supported by the Deanship of Scientific Research (DSR) of King Abdulaziz University, Jeddah, Saudi Arabia.

References

[1] Abbasbandy S, Hayat T. Solution of the MHD Falkner–Skan flow by Homotopy analysis method. Commun Nonlinear Sci Numer Simul 2009;14(9–10):3591–8.
[2] Abbasbandy S, Hayat T. Solution of the MHD Falkner–Skan flow by Hankel–Padé method. Phys Lett A 2009;373(7):731–4.
[3] Parand K, Rezaei AR, Ghaderi SM. An approximate solution of the MHD Falkner–Skan flow by hermite functions pseudospectral method. Commun Nonlinear Sci Numer Simul 2011;16:274–83.
[4] Yang GC, Lan KQ. The velocity and shear stress functions of the Falkner–Skan equation arising in boundary layer theory. J Math Anal Appl 2007;328:1297–308.
[5] Yao B. Approximate analytical solution to the Falkner–Skan wedge flow with the permeable wall of uniform suction. Commun Nonlinear Sci Numer Simul 2009;14(8):3320–6.
[6] Yao B. Series solution of the temperature distribution in the Falkner–Skan wedge flow by the homotopy analysis method. Eur J Mech B 2009;28(5):689–93.
[7] Anabtawi M, Khuri S. On the generalized Falkner–Skan equation governing boundary layer flow of a FENE-P fluid. Appl Math Lett 2007;20(12):1211–5.
[8] Zhu S, Wu Q, Cheng X. Numerical solution of the Falkner–Skan equation based on quasilinearization. Appl Math Comput 2009;215(7):2472–85.
[9] Yao B, Chen J. Series solution to the Falkner–Skan equation with stretching boundary. Appl Math Comput 2009;208(1):156–64.
[10] Alizadeh E, Farhadi M, Sedighi K, Kebria HRE, Ghafourian A. Solution of the Falkner–Skan equation for wedge by Adomian decomposition method. Commun Nonlinear Sci Numer Simul 2009;14:724–33.
[11] Choi SU. Enhancing thermal conductivity of fluids with nanoparticle. ASME J Dev Appl Non-Newton Flows, FED 231/MD 1995;66:99–105.
[12] Choi SU, Zhang ZG, Lockwood W, Grulke FE. Anomalously thermal conductivity enhancement in nanotube suspension. J Appl Phys Lett 2001;79:2252–4.
[13] Das SK, Choi SU, Yu W, Pardeep T. Nanofluids: science and technology. New Jersey: Wiley; 2007.
[14] Wang XQ, Mujundar AS. A review on nanofluids – part I: theoretical and numerical investigations. Br J Chem Eng 2008;25:613–30.
[15] Yacob NA, Ishak A, Pop I. Falkner–Skan problem for a static wedge or moving wedge in nanofluids. Int J Therm Sci 2011;50:133–9.
[16] Fallah APM, Moradi A, Hayat T, Hendi AA. Pareto optimization of nanofluids Falkner–Skan wedge flow using genetics algorithm based on neural network modelling. Proc IAM 2012;1(1):15–35.
[17] Khan WA, Hamad MA, Ferdows M. Heat transfer analysis for Falkner–Skan boundary layer nanofluid flow past a wedge with convective boundary condition considering temperature dependent viscosity. Proc IMechE, J Nanoeng NanoSyst 2012:1–9.
[18] Khan WA, Pop I. Boundary layer flow past a wedge moving in a nanofluid. J Math Probl Eng 2013:7. Article ID. 637285.
[19] Zhao YL, Liao S. HAM-based mathematica package BVPh 2.0 for nonlinear boundary value problems. In: Liao S, editor. Advances in the homotopy analysis method. World Scientific Press; 2013 [chapter 7].
[20] Liao S. On the homotopy analysis technique and its applications. PhD dissertation, Shanghai Jiao Tong University; 1992.
[21] Liao S. Beyond perturbation. Introduction to homotopy analysis method. Boca Raton: Chapman and Hall/CRC Press; 2003.
[22] Liao S. Homotopy analysis method in nonlinear differential equations. Heidelberg: Springer; 2012.
[23] Liao S. An optimal homotopy-analysis approach for strongly nonlinear differential equations. J Commun Nonlinear Sci Numer Simul 2010;15:2003–16.
[24] Yih KA. Uniform suction/blowing effect on forced convection about a wedge: uniform heat flux. Acta Mech 1998;28(3–4):173–81.
[25] White FM. Viscous fluid flow. 2nd ed. New York (NY, USA): McGraw-Hill; 1991.